

Supporting information

Visible-light-induced photooxidation-Povarov cascade reaction:
synthesis of 2-arylquinoline through alcohol and
N-benzylanilines under mild conditions via Ag/g-C₃N₄
nanometric semiconductor catalyst

Peng Wang,^a Xiaowen Wang,^a Xiyu Niu,^a Li Zhu,^{b,*} and Xiaoquan Yao^{a,*}

^a Department of Applied Chemistry, College of Material Science and Technology, Nanjing University of
Aeronautics and Astronautics, Nanjing 210016, PR China

^b Department of Chemistry, School of Pharmacy, Nanjing Medical University, Nanjing 211166, PR China

Fax: +86-25-52112626; Phone: +86-25-52112902; e-mail: yaoxq@nuaa.edu.cn

Table of contents

Preparation and characterization of catalyst	S2-S6
Experimental section	S7-S8
Characterization for compounds	S9-S14
References	S15
¹ H NMR and ¹³ C NMR spectrum of 2&3	S16-S36

1. Preparation and characterization of catalyst

1.1 Preparation of porous g-C₃N₄ ^[1]

The porous g-C₃N₄ was synthesized by a classical solvothermal process. Typically, 15 mmol of 1,3,5-trichlorotriazine and 7.5 mmol of melamine powders were put into a 100-mL Teflon-lined autoclave, which was then filled with acetonitrile up to 60% of the total volume. The mixture was stirred at 180 °C for 48 h, and then, the resulting sample was sequentially washed with acetonitrile, distilled water and absolute ethanol several times and dried at 60 °C for 12 h to get an orange powder as the final product.

1.2 Preparation of Ag/g-C₃N₄ nanocomposite ^[2]

In a typical procedure, porous g-C₃N₄ (427 mg), trisodium citrate (147 mg) and polyvinylpyrrolidone (PVP, 100 mg) were mixed with 50 mL of distilled water, and ultrasonicated for 10 min. The mixture was then stirred and heated for 0.5 h at 60 °C. With vigorous stirring, a solution of AgNO₃ (42.7 mg), PVP (100mg) and 50 mL of distilled water was added drop by drop, and then, the reaction mixture was stirred vigorously and heated at 60 °C for another 5 h. After cooling down, the Ag/g-C₃N₄ nanocomposite was separated by centrifugation. After washing with distilled water (3 × 5mL), anhydrous ethanol (3 × 5mL) and anhydrous ether (3 × 5 mL) in order, the material was dried in vacuum at 40 °C for 12 hours to give the final Ag/g-C₃N₄ nanocomposite.

1.3 Characterization of catalyst

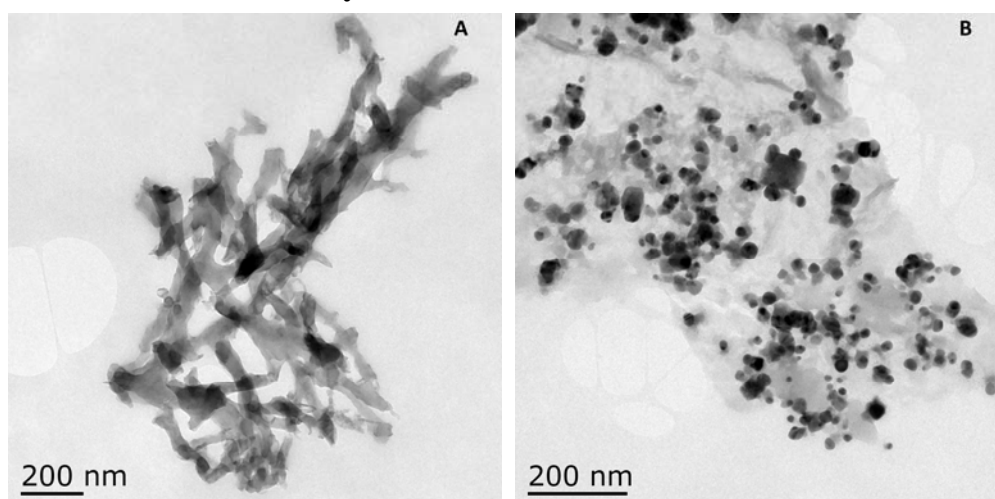


Figure S1. TEM images of A) g-C₃N₄, B) Ag/g-C₃N₄.

Figure S1A shows a TEM image of the porous g-C₃N₄ employed in our studies. As can be seen, g-C₃N₄ possessed a nanowire structure with homogeneous widths of about 50–60 nm

and lengths of the order of several micrometers. Ag nanoparticles (Ag NPs), which were prepared by a facile liquid-phase reduction method, were well anchored on g-C₃N₄ nanosheets;; Figure S1B indicates a relatively uniform size and shape of the Ag NPs, with the particle diameter of about 20-30 nm, generated on the surfaces of g-C₃N₄.

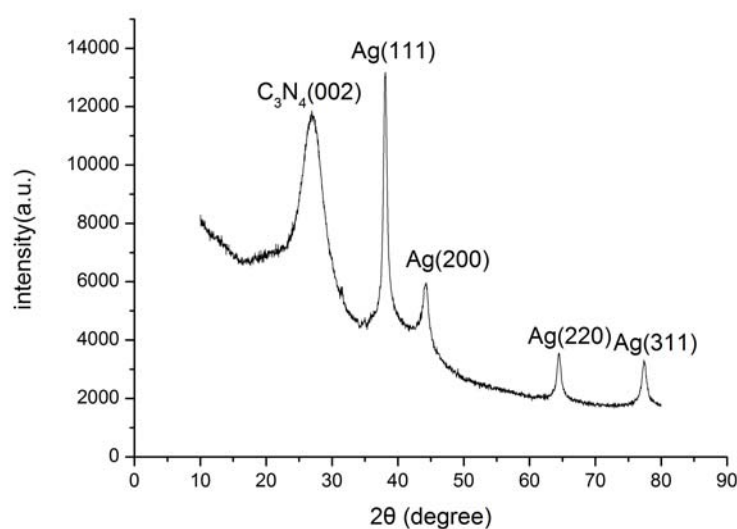


Figure S2. XRD patterns of the as-prepared Ag/g-C₃N₄.

XRD patterns of the as-prepared Ag/g-C₃N₄ composite and g-C₃N₄ are shown in Figure S2, the results confirmed graphitic-like layer structures in Ag/g-C₃N₄. The diffraction peaks at 28°[(002) diffraction plane] are the characteristic peaks of g-C₃N₄ (Figure S2), which can be attributed to the in-plane structural packing motif of tri-s-triazine units and the interlayer stacking of the conjugated aromatic system, respectively. The characteristic peaks of Ag NPs are at 38°, 44°, 65°, and 77° which can be attributed to the (111), (200), (220), and (311) lattice planes of metallic Ag, respectively. Such observations indicated that the Ag NPs were successfully loaded on the g-C₃N₄.^[2]

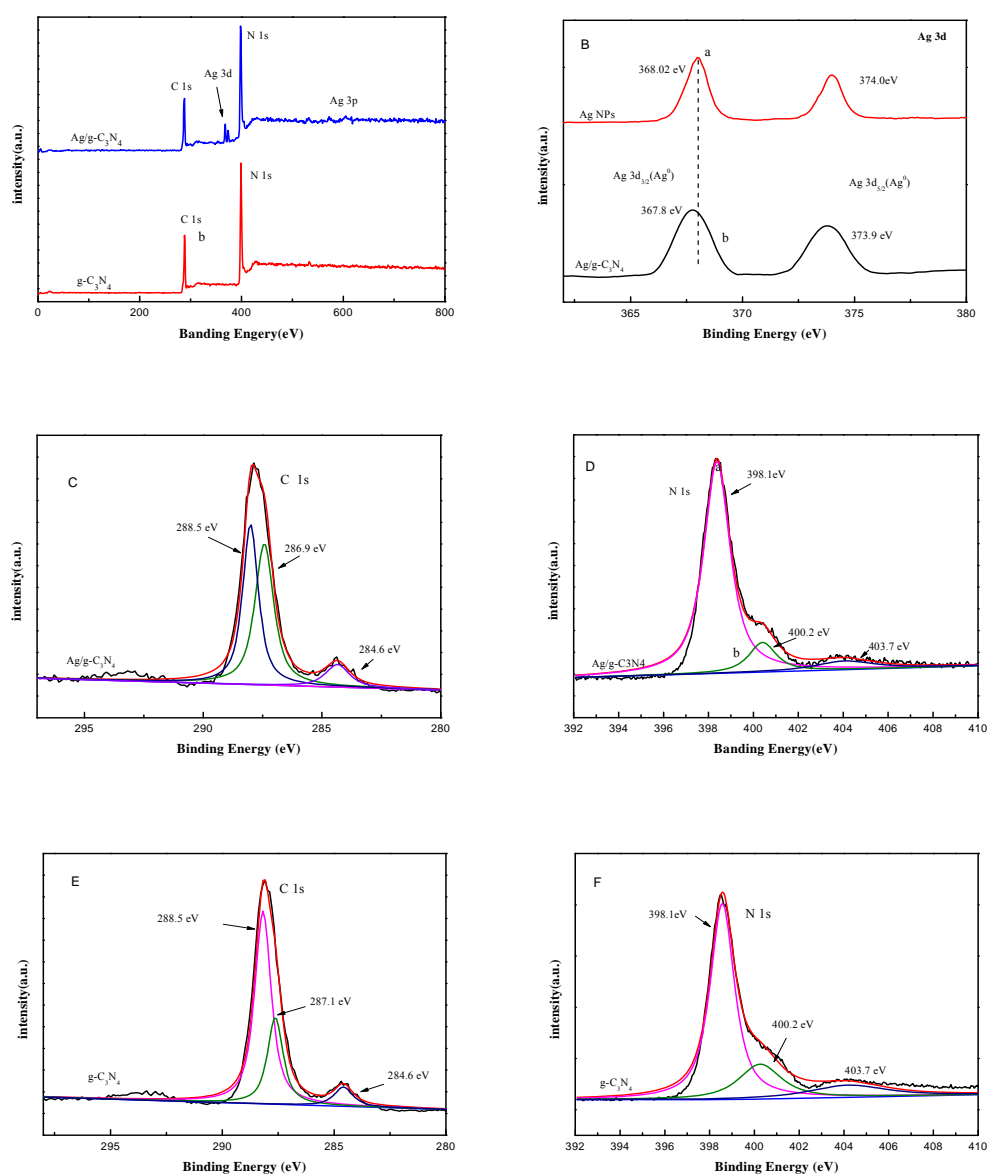


Figure S3. A) XPS survey spectra of the g-C₃N₄ and Ag/g-C₃N₄. B) High resolution XPS spectra Ag 3d. High resolution XPS spectra C1s (C) and N1s (D) of Ag/g-C₃N₄. High resolution XPS spectra C1s (E) and N1s (F) of g-C₃N₄.

Figure S3A shows the XPS survey spectra of the g-C₃N₄ and Ag/g-C₃N₄ nanocomposite. Comparing these spectra, new Ag peaks were observed, and the decoration of Ag nanoparticles on the g-C₃N₄ surface was further confirmed, which is in good agreement with the TEM results. The XPS Ag 3d spectrum of Ag/g-C₃N₄ and Ag NPs is shown in Figure S2B, in which the peaks at 367.8 and 373.9 eV are ascribed to Ag 3d_{3/2} [Ag(0)] and Ag 3d_{5/2} [Ag(0)] and the result is in accordance with previous reports.^[3] Moreover, the binding energy values of Ag 3d in Ag/g-C₃N₄ are slightly lower than those of Ag NPs. The shift might result from the strong interaction between Ag NPs and g-C₃N₄.

Figure S3C and D show the high resolution C1s and N1s spectra of the Ag/g-C₃N₄, which can be divided into three peaks, respectively. C1s at 286.9 eV and N1s at 398.1 eV are assigned to the sp² C=N bond in the s-triazine ring. The peaks at 288.5 eV and 284.6 eV in the C1s zone are attributed to electrons originating from an sp² C atom attached to an NH₂ group and to an aromatic carbon atom.^[1,4] The N1s peaks centered at 400.2 eV and 403.7 eV are ascribed to N atoms bonded to three C atoms [N-(C)₃] and the N atoms located in the heptazine ring and as bridging atom, respectively.^[1,4] The high resolution C1s and N1s spectra of the Ag/g-C₃N₄ are in agreement with those of g-C₃N₄ (Figure S2E and F), which indicated that after loading Ag nanoparticles, there were no significant changes to the graphitic C–N network.

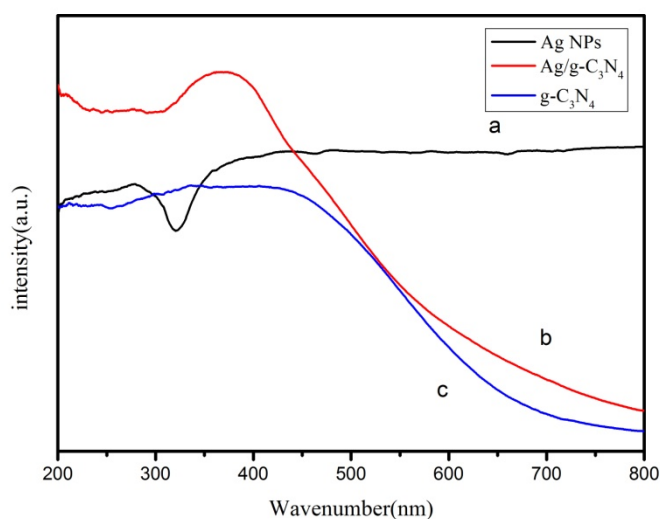


Figure S4. UV-vis diffuse reflectance spectra of g-C₃N₄, Ag NPs, and Ag/g-C₃N₄ nanocomposites.

Since the spectral absorption property of a photocatalyst is very important, UV-vis diffuse reflectance spectra (DRS) was used to examine the optical absorption properties of the photocatalysts. The UV-vis DRS of Ag NPs, Ag/g-C₃N₄ and g-C₃N₄ samples are demonstrated in Figure S4.

After loading Ag nanoparticles on the surface of g-C₃N₄, the absorption intensities of Ag/g-C₃N₄ composite became stronger in the whole spectrum window of interest, especially in the visible-light region, which might be due to the strong LSPR absorption of Ag nanocrystals and further confirmed the formation of Ag NPs.^[5] In addition, the absorption spectra were largely red-shifted, and a broad absorption ranging from 465 to 660 nm was detected. As for the as-prepared Ag NPs sample, it clearly exhibits a wide light absorption in

the whole UV-vis range of 200–800 nm. The results of UV-vis DRS show that the fabrication of the Ag/g-C₃N₄ composite can greatly improve the optical absorption property and increase the utilized efficiency of visible light, which is favorable for the enhancement of the photocatalytic activity.

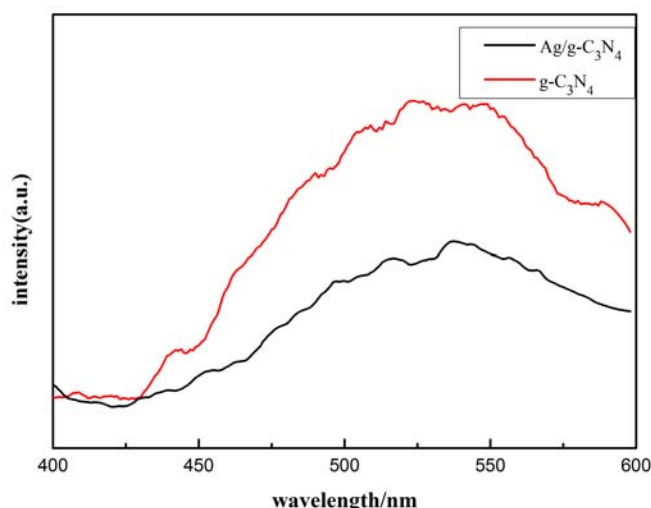


Figure S5. Photoluminescence (PL) spectra of g-C₃N₄ and Ag/g-C₃N₄ samples (excitation wavelength: $\lambda = 320$ nm)

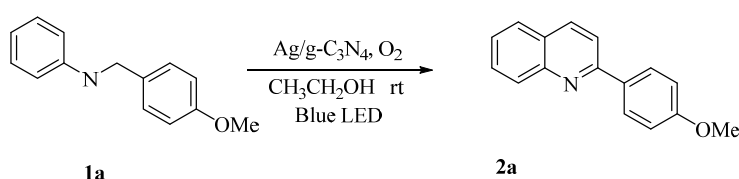
The recombination process of electron-hole pairs of semiconductors can release energy, which can be detected by PL emission. A lower photoluminescence intensity is a general indication of a lower recombination rate of electron-hole pairs, and usually results in higher photocatalytic activity.^[6]

Figure S5 shows the PL spectra of g-C₃N₄ and Ag/g-C₃N₄ samples excited at 320 nm. As can be seen from the figure, there is an obvious decrease in the PL intensity of Ag/g-C₃N₄ compared with that of g-C₃N₄. Notably, the much lower photoluminescence intensity of the Ag/g-C₃N₄ indicated that the separation of photogenerated electron-hole pairs in Ag/g-C₃N₄ was more efficient, because the excited electron could be transferred directly between the Ag NPs and g-C₃N₄ through their mutual interface.^[7] It might indicate that the Ag/g-C₃N₄ composite possessed higher photocatalytic activity under visible light irradiation than g-C₃N₄ or Ag Nps.

2. Experimental section

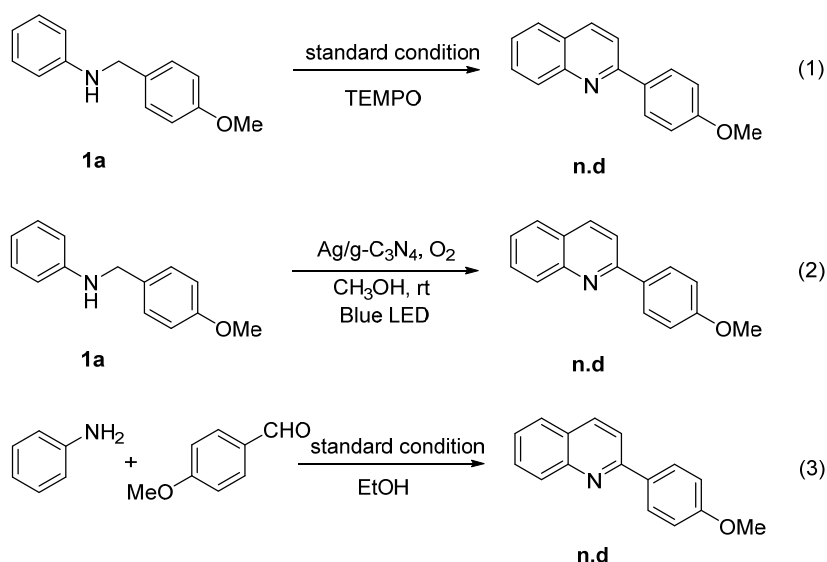
All experiments were carried out under oxygen atmosphere. Flash column chromatography was performed over silica gel 200-300 mesh. ^1H NMR spectra were acquired by 400 MHz, and ^{13}C NMR spectra were acquired by 101 MHz. Compounds **2p-2r** & **3a-3c** are unknown compounds and were characterized by ^1H & ^{13}C NMR, LR & HR MS. All of the known compounds described in the paper were characterized by comparing their ^1H & ^{13}C NMR to the previously reported data.

2.1 Typical procedures for the synthesis of 2-arylquinoline



N-(4-methoxybenzyl)aniline (**1a**, 0.1 mmol), 10% $\text{Ag/g-C}_3\text{N}_4$ (20 mol%) and alcohol (2 mL) were added into a 38 mL sealed tube under O_2 . The mixture was stirred at room temperature for 48 hours with 3W Blue LED irradiation. Then, the reaction mixture was concentrated by rotary evaporation, and the residue was purified by flash column chromatography on silica gel (hexanes : ethyl acetate = 20: 1). Compound **2a** was obtained in 78% of yield.

2.2 Some additional controlled experiments for the mechanism investigation.



Scheme S1. Some additional controlled experiments for the mechanism investigation.

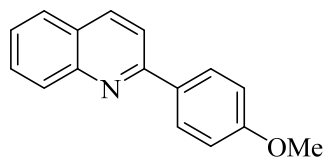
Under the standard reaction conditions, 1 equiv. of TEMPO was added as additive, and no reaction was observed. It is obviously that at least one step of the reaction should be involved

in a free radical process (Equation 1).

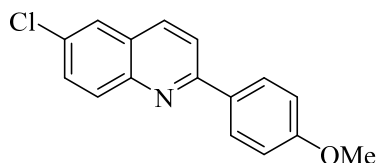
On the other hand, methanol was utilized as starting material instead of ethanol, and no any desired product was detected, only part of N-benzylaniline **1a** was decomposed. Compared with the standard reaction with ethanol, we proposed that the two carbons in 3 & 4-position of quinoline ring should be from ethanol (Equation 2).

Furthermore, 4-methoxybenzaldehyde (**1a**, 0.1 mmol), aniline (0.1 mmol) and ethanol (2 mL) were used as substrates, none of the target product was generated under the standard conditions. Based on this result and the similar phenomenon observed in entry 11, Table 1, we suspected that the free aniline can capture free radicals and inhibit the further reaction (Equation 3).^[13]

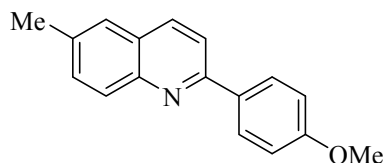
3. Characterization for compounds 2 & 3



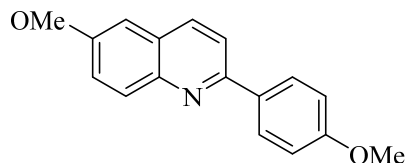
2-(4-methoxyphenyl)quinoline (2a, 78%):^[8] White solid. ¹H NMR (400 MHz, CDCl₃) δ 8.18-8.13(m, 4H), 7.84-7.78 (m, 2H), 7.70 (t, *J* = 7.2 Hz, 1H), 7.49 (t, *J* = 7.6 Hz, 1H), 7.05 (d, *J* = 8.8 Hz, 2H), 3.88 (s, 3H). ¹³C NMR (101 MHz, CDCl₃) δ 160.9, 157.0, 148.3, 136.7, 132.3, 129.6, 129.6, 128.9, 127.5, 127.0, 126.0, 118.6, 114.3, 55.4.



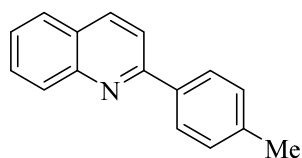
6-chloro-2-(4-methoxyphenyl)quinoline (2b, 82%):^[8] Yellow solid. ¹H NMR (400 MHz, CDCl₃) δ 8.12-8.03 (m, 4H), 7.81 (d, *J* = 8.7 Hz, 1H), 7.74 (d, *J* = 1.8 Hz, 1H), 7.63-7.60 (m, 1H), 7.03 (d, *J* = 8.7 Hz, 2H), 3.87 (s, 3H). ¹³C NMR (101 MHz, CDCl₃) δ 161.0, 157.1, 146.7, 135.7, 131.8, 131.5, 131.1, 130.5, 128.9, 127.5, 126.2, 119.4, 114.3, 55.4.



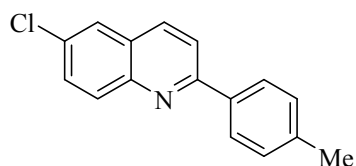
6-methyl-2-(4-methoxyphenyl)quinoline (2c, 63%):^[8] White solid. ¹H NMR (400 MHz, CDCl₃) δ 8.11 – 7.89 (m, 4H), 7.71 (d, *J* = 8.6 Hz, 1H), 7.46 (d, *J* = 11.7 Hz, 2H), 6.96 (d, *J* = 8.5 Hz, 2H), 3.80 (s, 3H), 2.46 (s, 3H). ¹³C NMR (101 MHz, CDCl₃) δ 160.7, 156.1, 146.9, 136.0, 135.8, 132.4, 131.9, 129.2, 128.8, 127.0, 126.4, 118.6, 114.2, 55.4, 21.6.



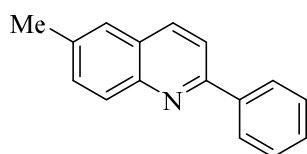
6-methoxy-2-(4-methoxyphenyl)quinoline (2d, 57%):^[8] White solid. ¹H NMR (400 MHz, CDCl₃) δ 8.13 – 8.01 (m, 4H), 7.79 (d, *J* = 8.6 Hz, 1H), 7.38-7.35 (m, 1H), 7.08 (d, *J* = 2.7 Hz, 1H), 7.04 (d, *J* = 8.8 Hz, 2H), 3.94 (s, 3H), 3.88 (s, 3H). ¹³C NMR (101 MHz, CDCl₃) δ 160.6, 157.5, 154.7, 144.3, 135.5, 132.4, 131.0, 128.6, 127.8, 122.2, 118.9, 114.2, 105.1, 55.6, 55.4.



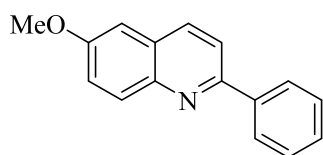
2-(4-methylphenyl)quinoline (2e, 73%):^[9] White solid. ¹H NMR (400 MHz, CDCl₃) δ 8.20-8.15 (m, 2H), 8.07 (d, *J* = 8.1 Hz, 2H), 7.87-7.80 (m, 2H), 7.71 (t, *J* = 7.6 Hz, 1H), 7.51 (t, *J* = 7.4 Hz, 1H), 7.33 (d, *J* = 7.9 Hz, 2H), 2.43 (s, 3H). ¹³C NMR (101 MHz, CDCl₃) δ 157.4, 148.3, 139.4, 136.9, 136.7, 129.7, 129.6, 127.5, 127.1, 126.1, 118.9, 21.4.



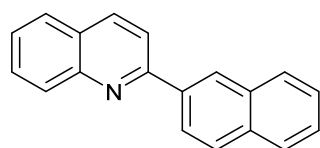
6-chloro-2-(4-methylphenyl)quinoline (2f, 71%):^[8] White solid. ¹H NMR (400 MHz, CDCl₃) δ 8.13 – 8.01 (m, 4H), 7.87 (d, *J* = 8.7 Hz, 1H), 7.78 (d, *J* = 2.3 Hz, 1H), 7.65-7.62 (m, 1H), 7.33 (d, *J* = 8.0 Hz, 2H), 2.43 (s, 3H). ¹³C NMR (101 MHz, CDCl₃) δ 157.6, 146.7, 139.8, 136.4, 135.8, 131.7, 131.3, 130.5, 129.7, 127.7, 127.4, 126.2, 119.7, 21.4.



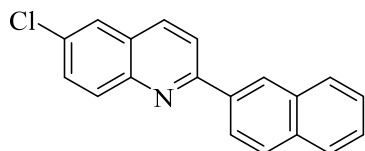
6-methyl-2-phenylquinoline (2g, 67%):^[10] White solid. ¹H NMR (400 MHz, CDCl₃) δ 8.18 – 8.03 (m, 4H), 7.81 (d, *J* = 8.6 Hz, 1H), 7.56-7.49 (m, 4H), 7.44 (t, *J* = 7.3 Hz, 1H), 2.53 (s, 3H). ¹³C NMR (101 MHz, CDCl₃) δ 156.6, 146.9, 139.9, 136.2, 136.1, 132.0, 129.5, 129.2, 128.9, 127.5, 127.3, 126.4, 119.0, 21.7.



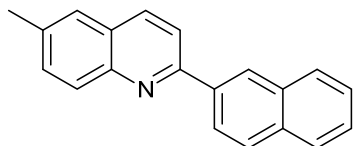
6-methoxy-2-phenylquinoline (2h, 61%):^[10] Yellow solid. ¹H NMR (400 MHz, CDCl₃) δ 8.17 – 8.03 (m, 4H), 7.82 (d, *J* = 8.5 Hz, 1H), 7.51 (t, *J* = 7.5 Hz, 2H), 7.43 (t, *J* = 7.3 Hz, 1H), 7.39-7.36 (m, 1H), 7.08 (d, *J* = 2.6 Hz, 1H), 3.93 (s, 3H). ¹³C NMR (101 MHz, CDCl₃) δ 157.7, 155.1, 144.4, 139.8, 135.6, 131.2, 129.0, 128.8, 128.2, 127.3, 122.4, 119.3, 105.1, 55.6.



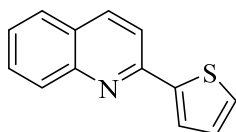
2-(naphthalen-2-yl)quinoline (2i, 63%):^[11] Yellow solid. ¹H NMR (400 MHz, CDCl₃) δ 8.62 (s, 1H), 8.37 (d, *J* = 8.6 Hz, 1H), 8.24 (dd, *J* = 11.8, 8.8 Hz, 2H), 8.04-7.99 (m, 3H), 7.91-7.89 (m, 1H), 7.85 (d, *J* = 8.1 Hz, 1H), 7.75 (t, *J* = 7.6 Hz, 1H), 7.56-7.52 (m, 3H). ¹³C NMR (101 MHz, CDCl₃) δ 157.2, 148.4, 137.0, 136.9, 133.9, 133.6, 129.8, 128.9, 128.6, 127.8, 127.6, 127.2, 126.8, 126.40, 125.1, 119.2.



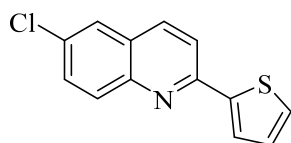
6-chloro-2-(naphthalen-2-yl)quinoline (2j, 83%):^[8] Yellow solid. ¹H NMR (400 MHz, CDCl₃) δ 8.58 (s, 1H), 8.33 (d, *J* = 8.6 Hz, 1H), 8.14-8.11 (m, 2H), 7.90-7.87 (m, 3H), 7.92 – 7.84 (m, 1H), 7.79 (d, *J* = 1.9 Hz, 1H), 7.67-7.65 (m, 1H), 7.54-7.51 (m, 2H). ¹³C NMR (101 MHz, CDCl₃) δ 157.3, 146.7, 136.5, 135.8, 134.0, 133.5, 131.9, 131.3, 130.6, 128.8, 128.6, 127.7, 127.2, 126.86, 126.4, 126.2, 124.9, 119.9.



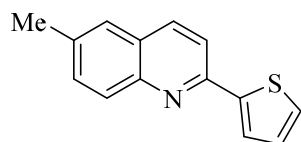
6-methyl-2-(naphthalen-2-yl)quinoline (2k, 75%):^[11] White solid. ¹H NMR (400 MHz, CDCl₃) δ 8.59 (s, 1H), 8.35 (dd, *J* = 8.6, 1.4 Hz, 1H), 8.12 (dd, *J* = 12.8, 8.5 Hz, 2H), 7.99-7.96 (m, 3H), 7.90 – 7.87 (m, 1H), 7.57 (d, *J* = 8.7 Hz, 2H), 7.52 (dd, *J* = 6.2, 3.2 Hz, 2H), 2.55 (s, 3H). ¹³C NMR (101 MHz, CDCl₃) δ 156.4, 147.0, 137.1, 136.3, 136.2, 133.8, 133.6, 132.1, 129.5, 128.9, 128.6, 127.8, 127.3, 127.0, 126.7, 126.4, 126.4, 125.1, 119.2, 21.7.



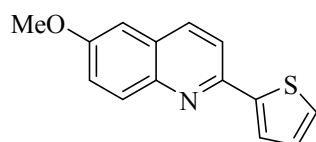
2-(thiophen-2-yl)quinoline (2l, 84%):^[12] White solid. ¹H NMR (400 MHz, CDCl₃) δ 8.05-8.00 (m, 2H), 7.71-7.59 (m, 4H), 7.41-7.38 (m, 2H), 7.10 – 7.03 (m, 1H). ¹³C NMR (101 MHz, CDCl₃) δ 152.4, 148.2, 145.5, 136.7, 129.9, 129.3, 128.6, 128.1, 127.5, 127.2, 126.1, 125.89, 117.7.



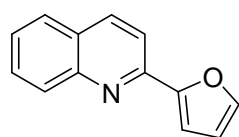
6-chloro-2-(thiophen-2-yl)quinoline (2m, 73%):^[8] White solid. ¹H NMR (400 MHz, CDCl₃) δ 7.91 (d, *J* = 8.6 Hz, 2H), 7.73 – 7.57 (m, 3H), 7.52 (d, *J* = 8.5 Hz, 1H), 7.38 (d, *J* = 4.1 Hz, 1H), 7.06 (s, 1H). ¹³C NMR (101 MHz, CDCl₃) δ 152.56, 146.5, 145.0, 135.7, 131.7, 130.8, 130.7, 129.0, 128.2, 127.7, 126.2, 126.2, 118.5.



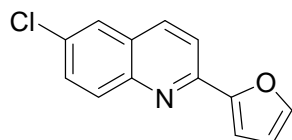
2-(thiophen-2-yl)-6-methoxyquinoline (2n, 66%):^[12] Yellow solid. ¹H NMR (400 MHz, CDCl₃) δ 8.03 (d, *J* = 8.6 Hz, 1H), 7.98 (d, *J* = 9.2 Hz, 1H), 7.75 (d, *J* = 8.6 Hz, 1H), 7.70 (d, *J* = 3.6 Hz, 1H), 7.52 (d, *J* = 6.9 Hz, 2H), 7.44 (d, *J* = 5.0 Hz, 1H), 7.15-7.13 (m, 1H), 2.52 (s, 3H). ¹³C NMR (101 MHz, CDCl₃) δ 151.6, 146.7, 145.6, 136.0, 136.0, 132.1, 129.0, 128.2, 128.1, 127.25, 126.5, 125.5, 117.7, 21.6.



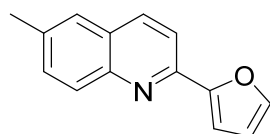
2-(thiophen-2-yl)-6-methoxyquinoline (2o, 53%):^[12] Yellow liquid. ¹H NMR (400 MHz, CDCl₃) δ 7.99 (t, *J* = 8.1 Hz, 2H), 7.73 (d, *J* = 8.6 Hz, 1H), 7.66 (d, *J* = 3.5 Hz, 1H), 7.42 (d, *J* = 5.0 Hz, 1H), 7.36-7.33 (m, 1H), 7.17 – 7.09 (m, 1H), 7.03 (d, *J* = 2.6 Hz, 1H), 3.91 (s, 3H). ¹³C NMR (101 MHz, CDCl₃) δ 157.6, 150.2, 145.6, 144.1, 135.4, 130.8, 128.2, 128.0, 127.9, 125.1, 122.4, 118.0, 105.3, 55.6.



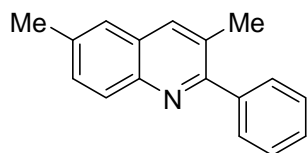
2-(naphthalen-2-yl)furan (2p, 71%): Yellow solid. ¹H NMR (400 MHz, CDCl₃) δ 8.14 (dd, *J* = 8.2, 4.7 Hz, 2H), 7.78 (dd, *J* = 16.2, 8.4 Hz, 2H), 7.70 (t, *J* = 7.6 Hz, 1H), 7.62 (s, 1H), 7.48 (t, *J* = 7.4 Hz, 1H), 7.21 (d, *J* = 2.9 Hz, 1H), 6.58 (d, *J* = 1.2 Hz, 1H). ¹³C NMR (101 MHz, CDCl₃) δ 153.7, 149.1, 148.1, 144.2, 136.7, 129.9, 129.4, 127.6, 127.2, 126.3, 117.5, 112.3, 110.2. MS (EI) *m/z* (%): 195(M⁺), 195(100), 167, 140, 128. HRMS calcd for C₁₃H₉NO: 195.0684, found 195.0690.



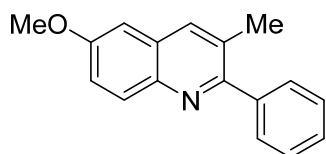
2-(6-chloronaphthalen-2-yl)furan (2q, 85%): Yellow solid. ^1H NMR (400 MHz, CDCl_3) δ 8.06 – 8.04 (m, 2H), 7.81 (d, J = 8.7 Hz, 1H), 7.74 (d, J = 2.0 Hz, 1H), 7.64-7.61 (m, 2H), 7.21 (d, J = 3.3 Hz, 1H), 6.60 – 6.59 (m, 1H). ^{13}C NMR (101 MHz, CDCl_3) δ 153.4, 149.2, 146.5, 144.4, 135.8, 131.8, 130.9, 130.8, 127.7, 126.3, 118.3, 112.4, 110.6. MS (EI) m/z (%): 229(M^+), 229(100), 201, 166, 139. HRMS calcd for $\text{C}_{13}\text{H}_8\text{ClNO}$: 229.0294, found 229.0295.



2-(6-methylnaphthalen-2-yl)furan (2r, 67%): Yellow solid. ^1H NMR (400 MHz, CDCl_3) δ 8.07 – 8.01 (m, 2H), 7.77 (d, J = 8.6 Hz, 1H), 7.61 (s, 1H), 7.53 (d, J = 4.6 Hz, 2H), 7.17 (d, J = 3.3 Hz, 1H), 6.58 (dd, J = 3.2, 1.6 Hz, 1H), 2.52 (s, 3H). ^{13}C NMR (101 MHz, CDCl_3) δ 153.8, 148.3, 146.7, 144.0, 136.2, 136.0, 132.2, 129.1, 127.2, 126.5, 117.5, 112.2, 109.7, 21.6. MS (EI) m/z (%): 209(M^+), 209(100), 180, 152, HRMS calcd for $\text{C}_{14}\text{H}_{11}\text{NO}$: 209.0841, found 209.0845

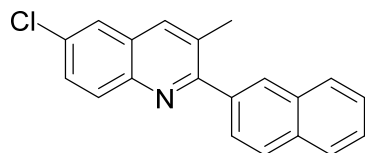


3,6-dimethyl-2-phenylquinoline (3a, 39%): Yellow liquid. ^1H NMR (400 MHz, CDCl_3) δ 8.01 (d, J = 8.6 Hz, 1H), 7.92 (s, 1H), 7.58 (d, J = 7.3 Hz, 2H), 7.53 (s, 1H), 7.48 (t, J = 7.5 Hz, 3H), 7.42 (t, J = 7.2 Hz, 1H), 2.54 (s, 3H), 2.45 (s, 3H). ^{13}C NMR (101 MHz, CDCl_3) δ 159.6, 145.3, 141.0, 136.2, 136.1, 131.0, 129.1, 129.0, 128.9, 128.3, 128.1, 127.6, 125.5, 21.6, 20.6; MS (EI) m/z (%): 233(M^+), 232(100), 217, HRMS calcd. for $\text{C}_{17}\text{H}_{15}\text{N}$: 233.1204; found 233.1202.



6-methoxy-3-methyl-2-phenylquinoline (3b, 43%): Yellow liquid. ^1H NMR (400 MHz, CDCl_3) δ 8.03 (d, J = 9.2 Hz, 1H), 7.92 (s, 1H), 7.57 (d, J = 7.0 Hz, 2H), 7.48 (t, J = 7.2 Hz,

2H), 7.42 (t, $J = 7.2$ Hz, 1H), 7.33-7.30 (m, 1H), 7.04 (d, $J = 2.6$ Hz, 1H), 3.94 (s, 3H), 2.45 (s, 3H). ^{13}C NMR (101 MHz, CDCl_3) δ 158.0, 157.8, 142.7, 140.9, 135.7, 130.7, 129.5, 128.9, 128.6, 128.3, 128.0, 121.5, 104.2, 55.5, 20.6; MS (EI) m/z (%): 249(M^+), 248 (100), 233, 217, 205, HRMS calcd for $\text{C}_{17}\text{H}_{15}\text{NO}$: 249.1154; found 249.1150.



6-chloro-3-methyl-2-(naphthalen-2-yl)quinoline (3c, 54%): White liquid. ^1H NMR (400 MHz, CDCl_3) δ 8.08 (d, $J = 9.5$ Hz, 2H), 7.97 (t, $J = 4.0$ Hz, 2H), 7.93 – 7.91 (m, 2H), 7.78 (d, $J = 1.7$ Hz, 1H), 7.71 (d, $J = 8.4$ Hz, 1H), 7.61 (dd, $J = 9.0, 1.9$ Hz, 1H), 7.55-7.53 (m, 2H), 2.52 (s, 3H). ^{13}C NMR (101 MHz, CDCl_3) δ 160.8, 145.1, 137.9, 135.9, 133.2, 133.2, 132.2, 131.0, 130.6, 129.8, 128.5, 128.3, 128.2, 128.1, 127.8, 126.6, 126.4, 125.5, 20.8; MS (EI) m/z (%): 303(M^+), 302 (100), 267, 239, 150, 132, HRMS calcd for $\text{C}_{20}\text{H}_{14}\text{ClN}$: 303.0815; found 303.0811.

Reference

- 1 Y. J. Cui, Z. X. Ding, X. Z. Fu and X. C. Wang, *Angew. Chem.*, 2012, **124**, 11984; *Angew. Chem. Int. Ed.*, 2012, **51**, 11814.
- 2 L. Wang, M. Yu, C. Wu, N. Deng, C. Wang and X. Yao, *Adv. Synth. Catal.*, 2016, **358**, 2631.
- 3 a) K. Tian, W. J. Liu and H. Jiang, *ACS Sustainable Chem. Eng.*, 2015, **3**, 269; b) L. Kuai, B. Geng, X. Chen, Y. Zhao and Y. Luo, *Langmuir*, 2010, **26**, 18723.
- 4 A. Thomas, A. Fischer, F. Goettmann, M. Antonietti, J. Muller, R. Schlogl and J. M. Carlsson, *J. Mater. Chem.*, 2008, **18**, 4893.
- 5 a) M. Zhu, P. Chen and M. Liu, *ACS Nano*, 2011, **5**, 4529; b) H. Cheng, B. Huang, P. Wang, Z. Wang, Z. Lou, J. Wang, X. Qin, X. Zhang and Y. Dai, *Chem. Commun.*, 2011, **47**, 7054.
- 6 X. Zhou, B. Jin, L. Li, F. Peng, H. Wang, H. Yu and Y. Fang, *J. Mater. Chem.*, 2012, **22**, 17900.
- 7 X. M. Lv, J. Y. Shen, Z. W. Wu, J. X. Wang and J. M. Xie, *J. Mater. Res.*, 2014, **29**, 2170.
- 8 X. Li, Q. Xing, P. Li, J. Zhao and F. Li, *E. J. Org. Chem.*, 2017, **3**, 618.
- 9 J. W. Yuan, L. R. Yang, P. Mao and L. B. Qu, *Org. Chem. Front.*, 2017, **4**, 545.
- 10 T. Demaude, L. Knerr and P. Pasau, *J. Comb. Chem.*, 2004, **6**, 768.
- 11 Arumugam V, Kaminsky W and Nallasamy D. *J. RSC Adv.*, 2015, **5(95)**: 77948.
- 12 (a) S. Sueki, C. Okamoto, I. Shimizu, K. Seto and Y. Furukawa, *Bull. Chem. Soc. Jap.*, 2010, **83**, 385; (b) M. Movassaghi and M. D. Hill. *J. Am. Chem. Soc.*, 2006, **128**, 4592.
- 13 (a) E. Pramauro, A. B. Prevot, V. Augugliaro and L. Palmisano, *Analyst*, 1995, **120**, 237; (b) M. I. Qadir, J. D. Scholten and J. Dupont, *Catal. Sci. Technol.*, 2015, **5**, 1459; (c) R. Levi, M. Milman, M. V. Landau, A. Brenner and M. Herskowitz, *Environ. Sci. Technol.*, 2008, **42**, 5165-5170; (d) H. Hao, L. Zhang, W. Wang and S. Zeng, *Catal. Sci. Technol.*, 2018, **8**, 1229.

^1H NMR and ^{13}C NMR spectrum of 2&3

